

Restored quantum size effects of Pb overlayers at high coverages

A. Ayuela,¹ E. Ogando,² and N. Zabala^{1,2}

¹*Donostia International Physics Center (DIPC) and Unidad Física de Materiales,
Centro Mixto CSIC-UPV/EHU, 20018 Donostia, Spain*

²*Elektrizitatea eta Elektronika Saila, Zientzia eta Teknologia Fakultatea, UPV-EHU, P.K. 644, 48080 Bilbao, Spain*

(Received 3 August 2006; revised manuscript received 14 November 2006; published 10 April 2007)

Abnormally large stability of Pb nanostructures grown on metallic or semiconductor substrates has been observed even for heights of about 30 monolayers. Using both density-functional theory calculations and analytical models, we demonstrate that the stability at even higher coverages ($N > 30$ ML) is supported by an extra second quantum beat pattern in the energetics of the metal film as a function of the number of atomic layers. This pattern is triggered by the butterflylike shape of the Fermi surface of lead in the (111) direction and supports the detection of stable magic islands of higher heights than measured up to now.

DOI: [10.1103/PhysRevB.75.153403](https://doi.org/10.1103/PhysRevB.75.153403)

PACS number(s): 73.21.Fg, 68.35.-p, 71.15.Mb

The literature of the last 20 years presents many examples of new structures in the nanometer scale. Their physical properties show a different behavior from the bulk due to quantum size effects (QSEs). The quantum oscillations in the stability of the nanostructures decay in amplitude as their size increases, and an open general question is the convergence of this behavior toward the bulk. Before reaching the bulk limit, modulations in the quantum oscillations of the stability are observed for atomic clusters¹ and nanowires.^{2–4} Also, these modulations are present in the growth of thin films, such as Pb layers, which is our topic in this paper.

Stability QSEs show up during the growth of Pb thin films^{5–10} because of the electronic confinement perpendicular to the substrate. Pb nanoislands over Cu(111) (Ref. 11) or Si(111) (Ref. 12) have revealed their preference for bilayer growth in the [111] orientation, first observed by Hinch *et al.*¹³ The origin of the “magic” height selection can be understood qualitatively with a simple picture of electrons confined in a potential well^{14,15} when looking to surface energies. In addition, the surface energy of the Pb film versus the number of monolayers (MLs) as seen in Fig. 1(a), shows a modulated pattern or quantum beat structure.^{16,17} In these works, the beat structure arises because the interlayer spacing is approximately $(3/4)\lambda_F$,^{16,17} where λ_F is the Fermi wavelength. Altogether, the previous works^{5–12,14–17} have always used only a single value of the Fermi wave vector of Pb. Nevertheless, a quantitative agreement with the measured magic heights requires more sophisticated models.

In fact, we are searching for extra modulations or quantum beats given by extra nestings of the Fermi surface. For layers, they have been studied in other context, such as sandwiched Co magnetic layers with a nonmagnetic Cu spacer.^{18–21} Both theoretical and experimental works discussed at length the role of the second Cu wave-vector nesting on the magnetic coupling between the sandwiched magnetic layers. However, the role of a second wave-vector nesting on the stability during the growth of layers has not been yet addressed.

In this paper, we explore larger sizes (up to 60 ML) of Pb thin films than usually researched in the literature by using the density-functional theory (DFT) and including the atomic structure. To study the stability of the films, we have calcu-

lated the energy as a function of the number of Pb MLs. Our main *ab initio* result is displayed in Fig. 2. We find that the oscillatory part of the energy as a function of the number of MLs has a second quantum beat structure that emerges from the nesting of two Pb Fermi wave vectors, as we will explain later. This second pattern affects the amplitude of these oscillations and explains the stability up to the calculated thickness of 60 ML. We are able to fit recent measurements up to 35 ML (Ref. 10) with a more sophisticated model that assumes two k_F values. Nevertheless, the effects of this second beat pattern emerge clearly just close to the thickness of 35 ML, so for a more extensive comparison, experiments in even higher coverages would be helpful.

Let us first summarize the main features for Pb islands, successfully modeled with the uniform jellium model in previous works.^{16,17} The oscillating part of the energy as a function of the Pb thickness is given in Fig. 1(a) with the full line. The minima of the curve correspond to the theoretically stable islands. Alternatively, one can look at (minus) the second derivative of the energy versus the thickness, the number of MLs (N), as shown in Fig. 1(b). The valleys are associated with the most stable sizes,^{9,10} as also studied in wires and clusters.²² The second derivative has been multiplied by the square of the effective thickness¹⁷ (D'^2) to show the damping of the amplitude within this model.

These oscillations and their decay using the jellium model assume implicitly only one Fermi wavelength; i.e., the Fermi surface is a circle in the direction perpendicular to the surface film. In this work, we address the question concerning stability at larger thicknesses ($N > 30$ ML) of the Pb slabs, when we allow for a second critical spanning vector of the Fermi surface. In the context of the present investigation, the second Fermi wavelength arises because the Fermi surface in the (111) direction is not perfectly circular but has a butterfly shape,^{11,23} as sketched in the inset of Fig. 3.

Jellium calculations describe the amplitude of the oscillations and their phase for a spherical Fermi surface. Therefore, in order to analyze the effect of the crystal structure with a realistic Fermi surface, we have calculated with DFT *ab initio* methods the energy as a function of thickness for the freestanding Pb slabs grown in the (111) direction. The calculations have been done with the VASP code²⁴ by using

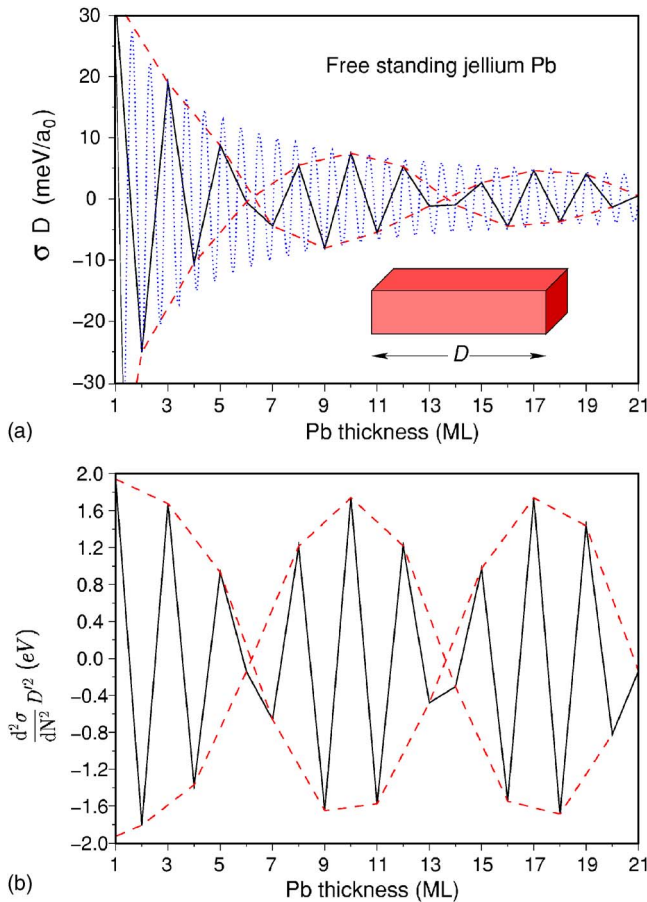


FIG. 1. (Color online) (a) Oscillating part of the total energy per surface area (σ) multiplied by the Pb slab effective thickness D' for a freestanding Pb, and calculated by means of self-consistent jellium calculations (Ref. 16). The dotted (blue/dark gray) line is a function of the continuous thickness, and the full (black) line connects the values of completed MLs. The dashed (red/gray) lines guide the eye to show the (first) beat pattern. (b) Second derivative of σ multiplied by the square of the effective thickness given by a full (black) line and its envelope function with a dashed (blue/dark gray) line.

the generalized gradient approximation²⁵ for the exchange-correlation potential and the projector augmented-wave method.²⁶ Computational details of our calculation are given in Ref. 27. We assume bulk distances between atoms.²⁸ For our purpose, it is unnecessary to relax the atomic positions because self-compression effects at the surface produce negligible changes in the energy.²⁹ Stress at the interface or interaction with the substrate produces a shift on the oscillating structure or slight differences affecting only to small thickness up to 10 ML. However, they do not change the qualitative behavior of the oscillations, so we neglect the substrate in this study.¹⁶ As we are interested in the stability of the slabs, we have calculated first the total energy as a function of the number of atomic layers N up to $N=60$, and then we have evaluated the second derivative of the energy versus the thickness as done before in Fig. 1(b). Our result is displayed in Fig. 2.

For small thickness ($N < 30$), the structure is similar to Fig. 1. There is no contradiction with previous simple mod-

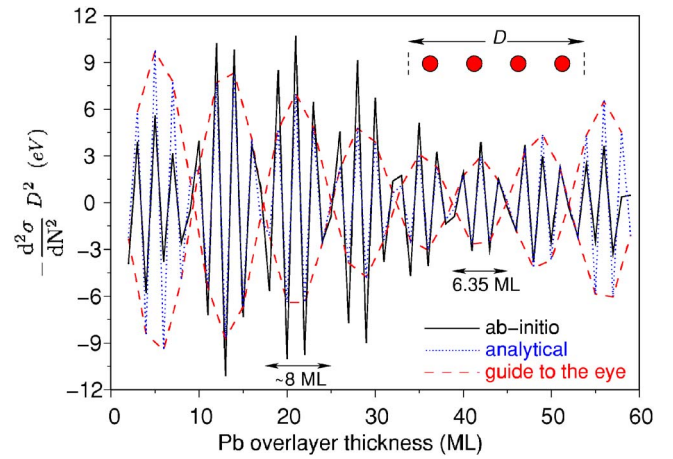


FIG. 2. (Color online) Second derivative of the energy per surface atom times the square of the Pb slab thickness versus the number of MLs (continuous line). The dotted (blue/dark gray) line is the analytical curve obtained with two values of the Fermi wavelengths $\lambda_1=7.47a_0$ and $\lambda_2=7.54a_0$ with weights $A_1=0.72$ and $A_2=1.28$, respectively. The dashed (red/gray) line is its envelope function.

els. Additionally, our central predictions are obtained when looking at the periods and decay of the oscillations at larger thickness. The amplitude of the oscillations, $-\frac{d^2\sigma}{dN^2}D^2$, in the $N=1-40$ range decays, while it remains constant for the jellium data, i.e., the *ab initio* results have stronger damping than the jellium results. Nevertheless, the amplitude for sizes larger than 40 ML remains constant. To our knowledge, experiments have not explored distances beyond this thickness, but our results indicate that oscillations would survive for larger sizes than explored currently up to now.

Also, a progressive shortening of the beat periods for large thicknesses ($N > 30$) is observed. Between $N=33$ and $N=39$, there is a non-negligible period change with a value of 6.35 ML.

These trends are reproduced analytically with a simple description as interference of two sinusoidal functions,

$$A_1 \sin[2k_1(dN + \delta_0)] + A_2 \sin[2k_2(dN + \delta_0)], \quad (1)$$

where k_1 and k_2 are the two nesting Fermi wave vectors in the [111] direction (see sketch in Fig. 3), A_1 and A_2 are their corresponding weights, δ_0 is a surface shift that accounts for the wave-function spill out at the slab walls, N is the number of atomic layers, and d is the interlayer spacing in the (111) direction. The *ab initio* calculations are in excellent agreement with the analytical model (dotted line in Fig. 2). In fact, the key point is that our *ab initio* calculations cannot be fitted using only one Fermi wave vector. Note that one Fermi wave vector is enough to fit the jellium results of Fig. 1(b). In summary, an extra nesting of the Fermi vectors is clearly involved in the mechanism to stabilize the Pb slabs.

Next, we compare our sum of sinusoidal functions, Eq. (1), and the experiments for supported Pb layers. We use Eq. (1) to fit the experimental results of Pb/Si(111).¹⁰ The energy oscillations are given in Fig. 3. The weights are $A_1=A_2=0.5$. It must be noticed that the position of the second

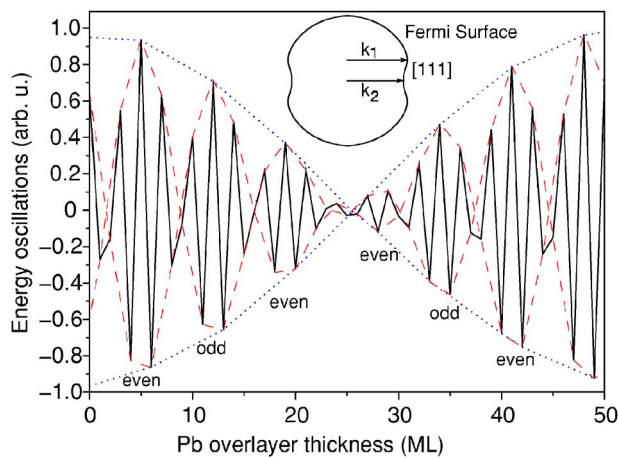


FIG. 3. (Color online) Modulated oscillatory pattern of the energy obtained by superposition of two oscillations following Eq. (1) and using the Fermi wavelength values $\lambda_1 = 7.40a_0$ and $\lambda_2 = 7.48a_0$, that are obtained by fitting the experimental curve (Ref. 10). The dashed (red/gray) line is the envelope of the first beat pattern and the dotted (blue/dark gray) line is the envelope of the second modulation, the so-called second beat pattern. The inset is a sketch of the cross section of the Fermi surface of Pb, showing both nesting vectors in the (111) direction.

quantum beat is inversely proportional to the difference of the wavelengths, so its determination is very sensitive to the input parameters. The Fermi wavelengths of the used vectors are very close to the free electron λ_F 's and to the values found in the literature for Pb [$\lambda_1 = 7.50$ a.u. and $\lambda_2 = 7.59$ a.u. with an experimental error around 0.1 a.u. (Ref. 11)]. The energy oscillations have beats every ≈ 8 ML, as it is known, but with a new modulation, the so-called second quantum beat which is at 29 ML. In Fig. 2, the absence of a clear second quantum beat is because $A_1 \neq A_2$. Although the largest thickness measured is around the second quantum beat position, our fitting reproduces completely the measured features, both oscillations and amplitudes. Again, the agreement using only one Fermi wave vector is worse. Theoretically, an additional hint of the double quantum beat comes out by the even-even successive regions intercalated in the even-odd alternation pattern of Fig. 3. This even-even characteristic appears at about $N = 29$. It seems to go unnoticed in

the already published experimental paper,¹⁰ where they have measured with x-ray diffraction up to $N \approx 35$ ML. With lower resolution, this even-even pattern is just in the experimental borderline. At this point, further experimental work is encouraged in order to look for such a second quantum beat pattern.

The decay of the amplitude of the energy smears out the energy oscillations at large thickness, so the size selection should disappear in experiments. Nevertheless, if this is accompanied by the second quantum modulation, we predict that they must emerge again at larger sizes. The observation of this effect in the stability is still an open question because the experiments did not go beyond that size. For example, the same effect of the nonspherical shape of the Fermi surface has been also pointed out to influence the magnetic interlayer coupling in multilayers, being important up to distances as long as 100 ML.^{30,31} This indicates that the detection of high stability with larger sizes would be possible in experiments.

In conclusion, both model and density-functional calculations show that there is a reentrance of QSEs and ensuing other features in the stability patterns at sizes substantially larger than the sizes studied up to now (or in the borderline). This suggests that the nesting with a second wave vector of the Fermi surface provides a mechanism to understand the stability at the large sizes in the growth of Pb layers. This second quantum beat claims for another interpretation of experiments, as well as for extra measurements at higher Pb coverages to shed light about the existence of the second quantum modulation and its role in the self-selection and self-assembly processes.

This work was supported by the ETORTEK (NANOMAT) program of the Basque government, Spanish Ministerio de Ciencia y Tecnología (MCyT) of Spain (Grant No. Fis 2004-06490-CO3-00), the European Network of Excellence NANOQUANTA (NM4-CT-2004-500198) and the Intramural Special Project (Ref. 2006601242). The SGI/IZO-SGIker UPV/EHU (supported by the National Program for the Promotion of Human Resources within the National Plan of Scientific Research, Development and Innovation-Fondo Social Europeo, MCyT and Basque Government) is gratefully acknowledged for allocation of computational resources.

¹O. Genzken and M. Brack, Phys. Rev. Lett. **67**, 3286 (1991).

²A. I. Yanson, I. K. Yanson, and J. van Ruitenbeek, Nature (London) **400**, 144 (1999).

³A. I. Yanson, I. K. Yanson, and J. M. van Ruitenbeek, Phys. Rev. Lett. **84**, 5832 (2000).

⁴A. I. Yanson, I. K. Yanson, and J. M. van Ruitenbeek, Phys. Rev. Lett. **87**, 216805 (2001).

⁵D.-A. Luh, T. Miller, J. J. Paggel, M. Y. Chou, and T.-C. Chiang, Science **292**, 1131 (2001).

⁶L. Floreano, D. Cvetko, F. Bruno, G. Bavdek, A. Cossaro, R. Gotter, A. Verdini, and A. Morgante, Prog. Surf. Sci. **72**, 135

(2003).

⁷L. Aballe, C. Rogero, and K. Horn, Surf. Sci. **518**, 141 (2002).

⁸M. Saito, T. Ohno, and T. Miyazaki, Appl. Surf. Sci. **237**, 80 (2004).

⁹M. H. Upton, C. M. Wei, M. Y. Chou, T. Miller, and T. C. Chiang, Phys. Rev. Lett. **93**, 026802 (2004).

¹⁰P. Czoschke, H. Hong, L. Basile, and T.-C. Chiang, Phys. Rev. Lett. **93**, 036103 (2004).

¹¹R. Otero, A. L. Vázquez de Parga, and R. Miranda, Phys. Rev. B **66**, 115401 (2002).

¹²M. Hupalo and M. C. Tringides, Phys. Rev. B **65**, 115406 (2002).

- ¹³B. J. Hinch, C. Koziol, J. P. Toennies, and G. Zhang, *Europhys. Lett.* **10**, 341 (1989).
- ¹⁴F. K. Schulte, *Surf. Sci.* **55**, 427 (1976).
- ¹⁵Z. Zhang, Q. Niu, and C.-K. Shih, *Phys. Rev. Lett.* **80**, 5381 (1998).
- ¹⁶E. Ogando, N. Zabala, E. V. Chulkov, and M. J. Puska, *Phys. Rev. B* **69**, 153410 (2004).
- ¹⁷E. Ogando, N. Zabala, E. V. Chulkov, and M. J. Puska, *Phys. Rev. B* **71**, 205401 (2005).
- ¹⁸S. S. P. Parkin, R. Bhadra, and K. P. Roche, *Phys. Rev. Lett.* **66**, 2152 (1991).
- ¹⁹M. T. Johnson, S. T. Purcell, N. W. E. McGee, R. Coehoorn, J. aan de Stegge, and W. Hoving, *Phys. Rev. Lett.* **68**, 2688 (1992).
- ²⁰P. Bruno and C. Chappert, *Phys. Rev. Lett.* **67**, 1602 (1991).
- ²¹D. M. Edwards, J. Mathon, R. B. Muniz, and M. S. Phan, *Phys. Rev. Lett.* **67**, 493 (1991).
- ²²J. A. Alonso and M. J. Lopez, *J. Cluster Sci.* **14**, 31 (2003).
- ²³J. R. Anderson and A. V. Gold, *Phys. Rev.* **139**, A1459 (1965).
- ²⁴G. Kresse and J. Furthmüller, *Comput. Mater. Sci.* **6**, 15 (1996); *Phys. Rev. B* **54**, 11169 (1996).
- ²⁵J. P. Perdew, K. Burke, and M. Ernzerhof, *Phys. Rev. Lett.* **77**, 3865 (1996).
- ²⁶G. Kresse and D. Joubert, *Phys. Rev. B* **59**, 1758 (1999).
- ²⁷Convergence of the energies versus plane-wave cutoff (237 eV), k mesh (22×22), and vacuum (10 ML) were chosen when requiring high accuracy. These values are in agreement with the reference, D. Yu and M. Scheffler, *Phys. Rev. B* **70**, 155417 (2004).
- ²⁸C. M. Wei and M. Y. Chou, *Phys. Rev. B* **66**, 233408 (2002).
- ²⁹G. Materzanini, P. Saalfrank, and P. J. D. Lindan, *Phys. Rev. B* **63**, 235405 (2001).
- ³⁰P. Bruno, *J. Phys.: Condens. Matter* **11**, 9403 (1999).
- ³¹E. Holmström, A. Bergman, L. Nordström, I. A. Abrikosov, S. B. Dugdale, and B. L. Györfy, *Phys. Rev. B* **70**, 064408 (2004).